UDC 616-001.17:546.47
DOI – https://doi.org/10.14300/mnnc.2021.16045
ISSN – 2073-8137

PRACTICAL APPLICATION OF EFFICIENCY ESTIMATION OF NANOSIZED ZINC OXIDE IN THE THERAPY OF BURN WOUNDS

Elbekyan K. S. [1], Blinov A. V. [2], Blinova A. A. [2], Fedota N. V. [3], Orobets V. A. [3], Serov A. V. [2]

[1] Stavropol State Medical University, Russian Federation
[2] North-Caucasus Federal University, Stavropol, Russian Federation
[3] Stavropol State Agrarian University, Russian Federation

ОЦЕНКА ЭФФЕКТИВНОСТИ ИСПОЛЬЗОВАНИЯ НАНОРАЗМЕРНОГО ОКСИДА ЦИНКА В ТЕРАПИИ ОЖОГОВЫХ РАН

К. С. Эльбекьян [1], А. В. Блинов [2], А. А. Блинова [2], Н. В. Федота [3], В. А. Оробец [3], А. В. Серов [2]

[1] Ставропольский государственный медицинский университет, Российская Федерация
[2] Северо-Кавказский федеральный университет, Ставрополь, Российская Федерация
[3] Ставропольский государственный аграрный университет, Российская Федерация

The efficiency assessment of nanosized zinc oxide (ZnO) as a component of a high-potency wound-healing ointment composition was performed. The ointment consisted of a hydrophilic methylcellulose base and 5 wt. % ZnO nanoparticles as an active substance. Nanosized ZnO was obtained by the sol-gel method. Commercial zinc ointment was used as a comparison sample. Planimetric studies were conducted on the effectiveness of burn-wound healing in white Wistar rats. Three cases were considered: wounds were treated using a pharmaceutical zinc ointment or the ointment with ZnO nanoparticles, or received no treatment. Histological studies of the effectiveness of wound healing on treatment with the ointment containing ZnO nanoparticles were also performed. The ointment with the nanosized ZnO-based composition based had a pronounced regenerative effect on burn wounds. Its effect was greater than that of the existing analog – pharmaceutical zinc ointment.

Keywords: zinc oxide nanoparticles, ointment, wound healing, burn injuries, regenerative effect

Проведена оценка эффективности наноразмерного оксида цинка в качестве компонента высокоэффективной ранозаживляющей мази. Мазь состояла из гидрофильной метилцеллюлозной основы и наночастиц ZnO в качестве активного вещества. Наноразмерный ZnO был получен золь-гель методом. В качестве образца сравнения была использована фармацевтическая цинковая мазь. Проведены планиметрические исследования эффективности заживления ожоговых ран у лабораторных белых крыс. Рассмотрены три вида обработки ран: обработка фармацевтической цинковой мазью, разработанной мазью с наночастицами ZnO и без какой-либо обработки. Кроме того, было проведено гистологическое исследование, показавшее эффективность заживления ран при лечении мазью с наночастицами оксида цинка. На основании проведенного исследования было установлено, что мазевая композиция на основе наноразмерного оксида цинка оказывает выраженное регенерирующее действие на ожоговую рану, включая сравнение с существующими мазевыми аналогами оксида цинка.

Ключевые слова: наночастицы оксида цинка, мазь, ранозаживление, ожоги, регенеративный эффект

For citation: Elbekyan K. S., Blinov A. V., Blinova A. A., Fedota N. V., Orobets V. A., Serov A. V. PRACTICAL APPLICATION OF EFFICIENCY ESTIMATION OF NANOSIZED ZINC OXIDE IN THE THERAPY OF BURN WOUNDS. *Medical News of North Caucasus.* 2021;16(2):194-199. DOI – https://doi.org/10.14300/mnnc.2021.16045

Для цитирования: Эльбекьян К. С., Блинов А. В., Блинова А. А., Федота Н. В., Оробец В. А., Серов А. В. ОЦЕНКА ЭФФЕКТИВНОСТИ ИСПОЛЬЗОВАНИЯ НАНОРАЗМЕРНОГО ОКСИДА ЦИНКА В ТЕРАПИИ ОЖОГОВЫХ РАН. *Медицинский вестник Северного Кавказа.* 2021;16(2):194-199. DOI – https://doi.org/10.14300/mnnc.2021.16045

MMPs – matrix metalloproteinases
NaCl – sodium chloride
S – wound area
SEM – scanning electron microscopy
ZnO – zinc oxide

Currently, biologically active nanosized materials are finding new applications and use in medicine because of their unique physicochemical properties and biofunctionality [1–4]. An example is nanoscale zinc oxide, which is an active component of many external-use treatment agents applied in both monotherapy and in combination with antibiotics in the treatment of dermatoses [5–8]. In addition to the fact that zinc is an essential trace element, and plays an extremely important role in the functioning

of the skin, zinc oxide meets several of the prerequisites for the treatment of burn wounds: zinc has anti-inflammatory properties [9–12]; zinc has a proven epithelizing ability and plays an important role in the healing process of wounds [13, 14]. This effect is mediated by several mechanisms. First, zinc-containing enzymes, matrix metalloproteinases (MMPs) and alkaline phosphatase, are required for the normal healing process. The activity of MMPs is significantly increased in the wound-healing process [15, 16], and these enzymes clean the wound of tissue detritus and modulate cell migration and extracellular matrix reconstitution [17]. Alkaline phosphatase is a marker of early-stage angiogenesis and is intrinsic to post-traumatic inflammation and connective tissue proliferation [18]; zinc also exhibits moderate antibacterial properties [19]. Although this element is a necessary micronutrient for prokaryote growth, at higher concentrations, it inhibits the growth of a number of bacteria; Gram-positive microorganisms are more sensitive to the inhibitory effect of zinc than Gram-negative [20].

With respect to the above, the purpose of this study is to investigate the biological activity of nanoscale zinc oxide (ZnO) and the possibilities of its practical application in the composition of wound healing ointment for burn wound therapy.

Material and Methods. Preparation of nanosized ZnO. Reagent grade chemicals, grade A glassware and distilled water with 1.5–5 μS/cm conductivity were used. Nanosized ZnO was obtained by the sol–gel method. Zinc acetate was used as a precursor because smaller ZnO particles are obtained using this compound [21], and because the acetic acid residue completely evaporates at lower gel drying temperatures (125–225 °C) [21] in comparison with sulfate and nitrate anions, which decompose at significantly higher temperatures (700–900 °C).

The process of nanosized ZnO synthesis included the following series of successive stages: 1) Preparation of 0.2 mol/l zinc acetate solution in distilled water; 2) Dropwise addition of 25% ammonia solution to the zinc acetate solution under vigorous stirring with a constant pH. The process was performed at approximately pH 8, because the formation of zinc oxide gel from its hydroxide was observed at this pH value ($Zn(OH)_2 \rightarrow ZnO + H_2O$); 3) Aging of the gel for 1 hour; 4) Centrifugation of the gel and washing with distilled water to eliminate ionic impurities; 5) Drying of the gel at 100 °C for 24 h; 6) Calcination of zinc oxide powder at 175 °C for 12 h.

Preparation of nano-ZnO-based ointment. The ointment composition included hydrophilic methylcellulose (MC-100) base and ZnO nanoparticles as an active substance. A hydrophilic ointment composition for the treatment of burns was prepared as follows: 1) The methylcellulose powder of 0.03 wt. % was mixed with distilled water and left to swell for 30–60 min; 2) The nanosized ZnO powder and glycerol were added to the formed methylcellulose gel under constant stirring; 3) The resulting mixture was homogenized for 2 h.

The mixture's quantitative composition was as follows: Nanosized ZnO – 5 wt. %; Glycerol – 5 wt. %; Methylcellulose – 0.03 wt. %; Distilled water – 89.97 wt. %.

The developed composition was a homogeneous white odorless ointment with a pH of approximately 7.

ZnO nano-powder morphology and phase composition. X-ray powder diffraction analysis was conducted using an X-ray Diffractometer Empyrean (PANalytical, Almeo, the Netherlands) to determine the phase composition of the nanoparticles. The parameters of the measurement were as follows: 1) Copper cathode (emission wavelength 1.54 Å); 2) Current 35 mA; 3) Voltage 40 kV; 4) 2θ measurement range 30–85°; 5) 2θ sampling rate: 0.01°.

Morphology of the ZnO nanoparticles was examined by scanning electron microscopy (SEM) using an MIRA3-LMH microscope with the element determination system AZtecEnergy Standart/X-max 20 (standard) (Tescan, Brno, Czech Republic).

Efficiency of burn wound healing. The experiments on the regenerative activity of the obtained ointment were performed on 60 white Wistar male rats weighing 170±20 g, obtained from the «Pushchino» laboratory animal nursery (Pushchino, Russian Federation). The animal studies were performed in compliance with the bioethical rules in accordance with Order No. 742 of the Ministry of Higher and Secondary Specialized Education of the USSR dated November 13, 1984 «On the approval of the Rules for conducting work with the use of experimental animals». The rats were housed individually and the feeding regime was identical for each group of the experiment. The studies were performed at the vivarium and approved by the local ethics committee of Stavropol State Agrarian University. The burn wound model was generated as described below. Following preliminary skin treatment, in aseptic conditions under short-term narcosis, the skin was cauterized on a shaven square interscapular site of skin with an area of 2.5 cm^2. Therefore, the shape, area and location of the wounds were the same for each tested animal, so that the dynamics of regeneration and wound healing could be directly compared. Three groups of animals were designated, each group containing 20 animals. In group 1, the surface of the burn wound was treated daily with the ointment containing nanosized ZnO, starting from the first day of wound modeling up to day 14. The rats in group 2 were treated analogically with a commercial zinc ointment (Rosvetfarm, Russian Federation, TU 9318-009-16923913-01). The burn wounds of the animals of group 3 were treated with an isotonic saline solution (0.9 % NaCl) as controls.

The planimetric method proposed by Popova et al. [22] was used to obtain the objective indices of wound healing. The method is based on the determination of wound area reduction over time. Measurements of the burn wound model were performed on days 1, 3, 5, 10 and 14.

To analyze the dynamics of burn wound regeneration in detail, the following parameters were calculated for the animals in each group:

The daily percentage reduction of the wound area was calculated as follows:

$$\vartheta = \frac{(S - S_n)}{S \cdot t},$$

where S is the wound area at the previous measurement, cm^2;
S_n is the wound area at the current measurement, cm^2;
t is the number of days between the previous and current measurements.

The healing rate was calculated using the formula:

$$U = \frac{(S - S_n)}{n},$$

where S is the wound area at the previous measurement, cm^2;
S_n is the wound area at the current measurement, cm^2;
n is the number of days.

The mean healing rate of burn wounds was calculated as follows:

$$U_{cp} = \frac{(S_n - S_k)}{n},$$

where S_n is the wound area at the current measurement, cm^2;

S_k is the wound area at the end of the experiment;
n is the duration of the experiment, days.

At the end of the experiment, rats were euthanized via inhalation of 96% diethyl ether so that the structure of the brain and visceral system organs could be studied.

Histological material was taken on days 1, 5 and 7 after the simulation of burn wounds. For histological studies, tissue sections of 1.0×0.3 cm were made, which were then placed in 10% formalin solution for 2 h [23, 24]. The material was consequentially kept in six solutions of isopropyl alcohol with increasing concentrations for one hour in each and then placed in homogenized histological paraffin «Histomix» for 4 h at 62 °C, regulated by thermostat. The material prepared in this way was inserted into histological cassettes. Paraffin sections with a thickness of 0.5 mm were made using a microtome and pasted on histological glasses. Histological sections were stained with hematoxylin and eosin [25]. Digital images of each preparation were taken using an Axio Lab.A1 microscope (Carl Zeiss, Jena, Germany). For statistical processing the Statistica 10.0 program (StatSoft, USA) was used with parametric (Student's t-test) and nonparametric (Wilcoxon's W test) tests.

Results and Discussion. The structure and phase composition of the obtained nanosized ZnO was investigated by X-ray diffraction. The diffractogram is presented in Figure 1.

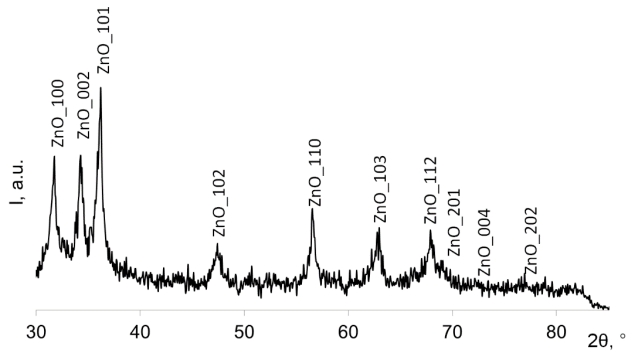

Fig. 1. Diffractogram of nanosized ZnO, calcined at 175 °C

As shown in Figure 1, the diffractogram of nanosized ZnO include all the characteristic peaks of wurtzite. The peaks are broad and have a low intensity. These data confirm the fact that the synthesized ZnO nanoparticles were finely dispersed. Additionally, SEM of the synthesized zinc oxide was performed. The SEM microphotographs are presented in Figure 2. The synthesized ZnO nanoparticles were quasi-spherical and had a mean size of approximately 30 nm.

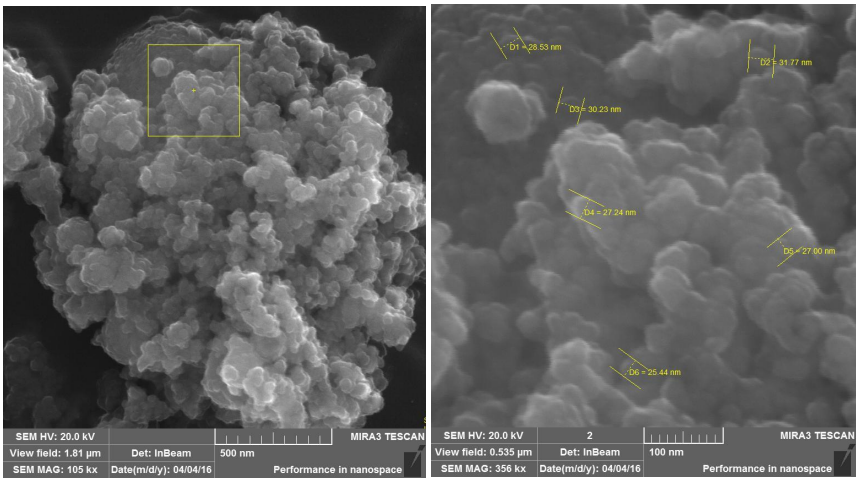

Fig. 2. SEM images of synthesized zinc oxide nanoparticles

The kinetic curves of model wound area reduction for each group of rats were plotted (Fig. 3). Data analysis showed that the mean wound area decreased in all groups after the first day of wound modeling. Moreover, the area of burn wounds displayed a decrease during the entire experiment for each test group. Analysis of wound area kinetic curves revealed that the rate of wound area reduction was greatest in the first group of rats, which were treated with the designed ointment based on ZnO nanoparticles.

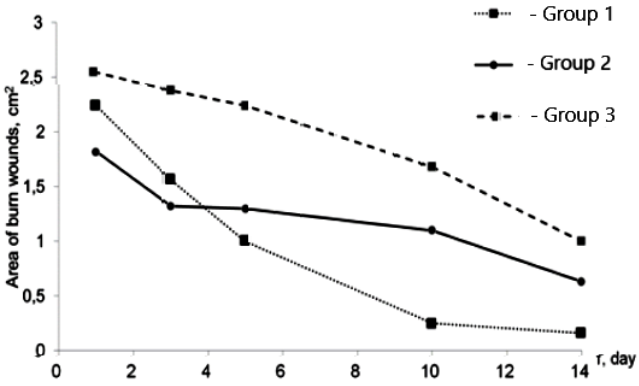

Fig. 3. The kinetic curves of model wound area reduction for test groups 1 and 2 and control group 3

The degree of burn wound healing of the animals in the first group was 27.48% and 32.08% greater in comparison with the second and control groups, respectively.

The results of the calculation of daily wound area reduction are presented in Figure 4.

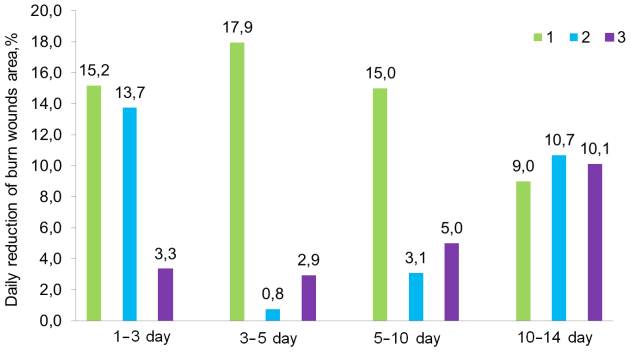

Fig. 4. Daily reduction of the burn wound area for animals in group 1, group 2 and control group 3

The data demonstrated that the developed nanoparticle ZnO ointment composition promotes reduction of the wound area after the first day after application.

Images illustrating the healing wounds under the different treatment conditions are presented in Figure 5.

From day 3 to day 5 of treatment, the animals of group 1 demonstrated a 17.9 % decrease in the wound area (22 and 6 times more compared with groups 2 and 3, respectively). From day 5 to day 10 of treatment, the wound area in group 1 decreased by 15 %, which was five and three times more compared with groups 1 and 2, respectively. Finally, from day 10 to day 14 of treatment, the wound area

reduction was approximately equal for each group. The wounds in group 1 were almost completely healed by the end of the experiment.

The data obtained show that the rate of wound healing in group 1 was the highest for each stage of the experiment. From day 1 to day 3 of treatment, the healing rate was 0.34 cm^2 per day in group 1, which was 1.36 and 3.78 times higher than in groups 2 and 3, respectively. From day 3 to day 5 of treatment, the healing rate in group 1 was 0.28 cm^2 per day, which was 28 and 4 times greater than that in groups 2 and 3, respectively. During this stage of treatment, the healing rate in group 2 was approximately zero. From day 5 to day 10 of treatment, the healing rate of burn wounds in group 1 was 0.15 cm^2 per day, which was 3.75 and 1.36 times greater than that in groups 2 and 3, respectively.

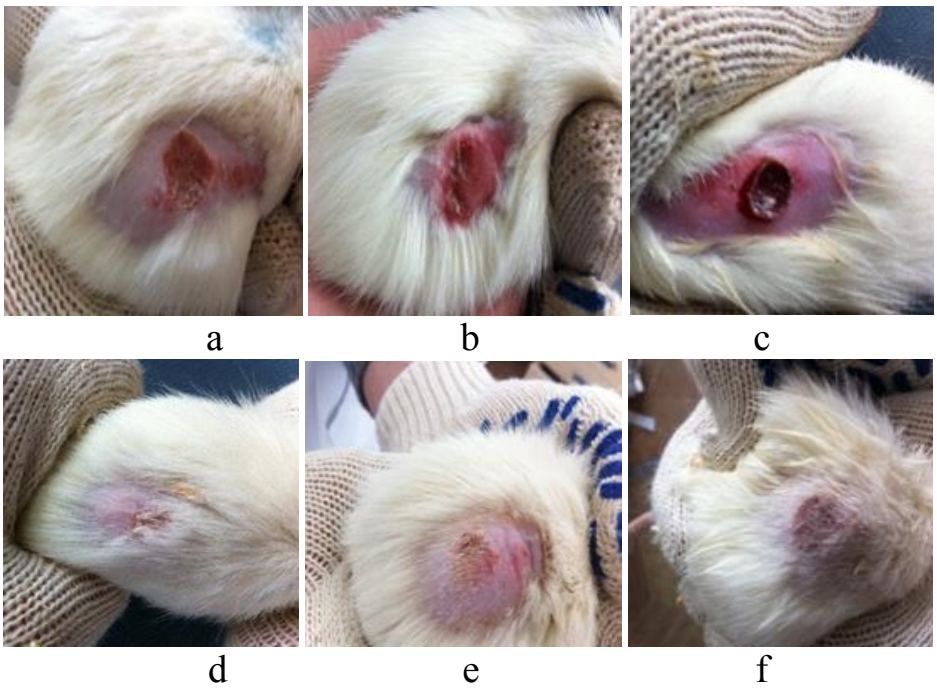

Fig. 5. Images of burn wounds on day 5 of treatment: a) group 1, b) group 2, c) group 3, and on day 10 of treatment: d) group 1, e) group 2, f) group 3

The rate of burn wound healing calculated for the entire experiment in group 1 was 1.78 and 1.33 times higher than in the groups 2 and 3, respectively.

For an objective assessment of the developed ointment composition effectiveness in the burn wound treatment, in addition to the results of a planimetric study, it is necessary to conduct morphological studies. In this regard, as part of the present study, a histological analysis of damaged tissue fragments in the area of thermal burn was performed.

In animals of group 3, a large, fragmented scab partially covered the wound, and in some cases it was separated from the underlying tissues of the wound. In the center of the wound, mature granulation tissue was present containing various hematogenous and tissue cellular elements; isolated macrophages, fibroblasts and collagen fibers were observed on the wound edges. Additionally, growth of the newly formed epithelium was observed, with the length of the regenerated tissue of 574.51±12.46 versus 589.01±14.58 μm in group 1; on the border with intact epidermis, hypertrophy was detected.

Fragments of the scab remained in the center of wound in group 3 after 5 days from the start of the treatment. A small area of granulation tissue containing round-cell elements was localized under the scab. The epithelium was sharply hypertrophied at the border with intact skin; the regenerated tissue was distinguished by the formation of small outgrowths of the basal membrane into the underlying tissue. Where wounds were treated with isotonic solution, partial or complete epithelization of the damaged areas occurred simultaneously in the animals of the control group. In individual rats, a flat epithelial layer, consisting of 8–10 rows of cells with a flat basal membrane, which did not form outgrowths in the thickness of the dermis, was formed on the surface of the wound. Its length was 164.4±8.01 versus 226.13±6.95 μm in group 1 ($p<0.05$). Under the epithelium, the wound defect was filled with mature granulation tissue with pronounced vascularization and a characteristic horizontal arrangement of fibroblasts around the vessels.

After 7 days, the differences we noted earlier appeared most clearly. In animals of groups 1 and 2, complete epithelialization of the damaged areas was observed. The newly formed epithelial layer, consisting of several rows of cells, covered the entire area of the defect. Although the basal membrane had an uneven configuration, no outgrowths into the underlying tissue were observed and the formation of hair follicles and sebaceous glands did not occur. Connective tissue with typical cellular structures was located under the epithelium. In group 3, the wound process was completed with the formation of organ-specific regenerated tissue. This was shown by complete wound epithelization and significant contraction of the damaged area, which was demonstrated by a shorter regeneration duration (609.22±15.01 in group 1 versus 634.72±18.01 μm in group 3), hair follicles and sebaceous gland growth.

Conclusions. The analysis of wound area reduction over time showed that the ointment composition containing nanosized ZnO displayed high regenerative efficiency; this effect was significantly greater than that of the pharmaceutical zinc ointment. On treatment with the designed ointment with ZnO nanoparticles, the reduction rate of the burn wound area during the first 3 days was almost five times greater in comparison with the control group and almost 1.5 times greater compared with the group treated with pharmaceutical zinc ointment. These results confirm the effective action of ZnO nanoparticles during the inflammatory stage, comprising wound cleaning, macrophage migration to the wound site and activation of collagen synthesis by fibroblasts. Additionally, the antibacterial properties of the ZnO nanoparticles reduced the secondary infection of wounds, supporting efficient and functional wound healing [26–29].

The application of nanosized ZnO with a high surface area as a component of a developed ointment composition allows the enrichment of the wound cells with zinc ions. Because of normalization of the zinc inflow to the wound cells, the rate of DNA replication, limited by thymidine kinase, is maintained.

Histological studies demonstrated the effectiveness of the ointment with nanosized ZnO in the treatment of skin wounds by improved healing (*per primam intentionem*). The inclusion of ZnO nanoparticles in the ointment led to a reduced level of inflammation, which is a morphological indicator for granulation tissue formation in the damaged area. Active angiogenesis and fibroblast proliferation accompanying granulation tissue formation and its subsequent transformation into connective tissue, and an increase in the rate of epithelialization of the damaged area are essentially a reflection of the transition of wound healing from the inflammatory phase to the proliferative phase.

Experimental animal procedures. The maintenance and care of experimental animals corresponded to the standards given in the Order of the Ministry of Health of the Russian Federation No. 708n of 23.08.2010 «On Approval of the Rules of Laboratory Practice in the Russian Federation» and the ethical principles established by the European Convention for the Protection of Vertebrates Used for Experimental and Other Scientific Purposes (adopted in Strasbourg on March 18, 1986 and confirmed in Strasbourg on June 15, 2006) and the positive conclusion of the local ethics committee. The study was approved by the local ethics committee.

Financial support. The research is carried out with the financial support of the Federal State Budget Institution «Fund of Assistance to Small Innovative Enterprises in sphere of Science and Technology», contract 11019GU/2016 of 13.02.2017.

Disclosures: The authors declare no conflict of interest.

Acknowledgments. We thank Edanz (https://www.edanz.com/ac) for editing a draft of this manuscript.

References

1. Mishra P. K., Mishra H., Ekielski A., Talegaonkar S., Vaidya B. Zinc oxide nanoparticles: A promising nanomaterial for biomedical applications. *Drug Discov. Today.* 2017:6446. https://doi.org/10.1016/j.drudis.2017.08.006
2. Sardella D., Gatt R., Valdramidis V. P. Physiological effects and mode of action of ZnO nanoparticles against postharvest fungal contaminants. *Food Res. Int.* 2017;101:274-279. https://doi.org/10.1016/j.foodres.2017.08.019
3. Gutha Y., Pathak J. L., Zhang W., Zhang Y., Jiao X. Antibacterial and wound healing properties of chitosan/poly(vinyl alcohol)/zinc oxide beads (CS/PVA/ZnO). *Int. J. Biol. Macromol.* 2017;103:234–241. https://doi.org/10.1016/j.ijbiomac.2017.05.020
4. Bae Y. S., Hill N. D., Bibi Y., Dreiher J., Cohen A. D. Innovative uses for zinc in dermatology. *Dermatol. Clin.* 2010;28:587-597. https://doi.org/10.1016/j.det.2010.03.006
5. Agarwal H., Kumar S. V., Rajeshkumar S. A review on green synthesis of zinc oxide nanoparticles – An eco-friendly approach. *Resour. Technol.* 2017;3(4):406-413. https://doi.org/10.1016/j.reffit.2017.03.002
6. Sonia S., Linda J. K. H., Ruckmani K., Sivakumar M. Antimicrobial and antioxidant potentials of biosynthesized colloidal zinc oxide nanoparticles for a fortified cold cream formulation: A potent nanocosmeceutical application. *Materials Science and Engineering.* 2017;79:581-589. https://doi.org/10.1016/j.msec.2017.05.059
7. Rakhshaei R., Namazi H. A potential bioactive wound dressing based on carboxymethyl cellulose/ZnO impregnated MCM-41 nanocomposite hydrogel. *Mater. Sci. Eng. C.* 2017;73:456-464. https://doi.org/10.1016/j.msec.2016.12.097
8. Raguvaran R., Manuja B. K., Chopra M., Thakur R., Anand T. [et al.] Sodium alginate and gum acacia hydrogels of ZnO nanoparticles show wound healing effect on fibroblast cells. *Int. J. Biol. Macromol.* 2017;96:185-191. https://doi.org/10.1016/j.ijbiomac.2016.12.009
9. Olbert M., Gdula-Argasinska J., Nowak G., Librowski T. Beneficial effect of nanoparticles over standard form of zinc oxide in enhancing the anti-inflammatory activity of ketoprofen in rats. *Pharmacol. Reports.* 2017;69:679-682. https://doi.org/10.1016/j.pharep.2017.02.004
10. Nagajyothi P. C., Cha S. J., Yang I. J., Sreekanth T. V. M., Kim K. J. [et al.] Antioxidant and anti-inflammatory activities of zinc oxide nanoparticles synthesized using Polygala tenuifolia root extract. *J. Photochem. Photobiol. B. Biol.* 2015;146:10-17. https://doi.org/10.1016/j.jphotobiol.2015.02.008
11. Mirzaei H., Darroudi M. Zinc oxide nanoparticles: Biological synthesis and biomedical applications. *Ceram. Int.* 2017;43:907-914. https://doi.org/10.1016/j.ceramint.2016.10.051
12. Lu Z., Gao J., He Q., Wu J., Liang D. [et al.] Enhanced antibacterial and wound healing activities of microporous chitosan-Ag/ZnO composite dressing. *Carbohydr. Polym.* 2017;156:460-469. https://doi.org/10.1016/j.carbpol.2016.09.051
13. Khalid A., Khan R., Ul-Islam M., Khan T., Wahid F. Bacterial cellulose-zinc oxide nanocomposites as a novel dressing system for burn wounds. *Carbohydr. Polym.* 2017;164:214-221. https://doi.org/10.1016/j.carbpol.2017.01.061
14. Jarrousse V., Castex-Rizzi N., Khammari A., Charveron M., Dreno B. Zinc salts inhibit in vitro Toll-like receptor 2 surface expression by keratinocytes, *Eur. J. Dermatology.* 2007;17:492-496. https://doi.org/10.1684/ejd.2007.0263
15. Lansdown A. B. G., Mirastschijski U., Stubbs N., Scanlon E., Agren M. S. Zinc in wound healing: Theoretical, experimental, and clinical aspects. *Wound Repair Regen.* 2007;15:2-16. https://doi.org/10.1111/j.1524-475X.2006.00179.x
16. Tarakanov V. A., Minaev S. V., Kolesnikov E. G., Korotkov K. G., Abushkevich V. G. [et al.] Topical diagnosis of the boundaries of necrotic segment of the small intestine in the high frequency electromagnetic fields. *Medical News of North Caucasus.* 2019;14(2):308-311. https://doi.org/10.14300/mnnc.2019.14074
17. Soo C., Shaw W. W., Zhang X., Longaker M. T., Howard E. W., Ting K. Differential expression of matrix metalloproteinases and their tissue-derived inhibitors in cutaneous wound repair. *Plast. Reconstr. Surg.* 2000;105:638-647.
18. Ravanti L., Kahari V. M. Matrix metalloproteinases in wound repair (review). *Int. J. Mol. Med.* 2000;6:391-407. https://doi.org/10.3892/ijmm.6.4.391
19. Alpaslan G., Nakajima T., Takano Y. Extracellular alkaline phosphatase activity as a possible marker for wound healing: a preliminary report. *J. Oral Maxillofac. Surg.* 1997;55:53-56.
20. Soderberg T., Hallmans G., Agren M., Tengrup I., Banck G. The effects of an occlusive zinc medicated dressing on the bacterial flora in excised wounds in the rat. *Infection.* 1989;17:81-85. https://doi.org/10.1007/BF01646881
21. Pourrahimi A. M., Liu D., Pallon L. K. H., Andersson R. L., Martínez A. [et al.] Water-based synthesis and cleaning methods for high purity ZnO nanoparticles – comparing acetate, chloride, sulphate and nitrate zinc salt precursors. *RSC Adv.* 2014;4:35568-35577. https://doi.org/10.1039/C4RA06651K
22. Gladkova E. V., Babushkina I. V., Mamonova I. A., Matveeva O. V., Belova S. V. Effect of a complex preparation on regeneration of the experimental soft tissue wound. *World J. Med. Sci.* 2013;8:226-230. https://doi.org/10.5829/idosi.wjms.2013.8.3.7364
23. Minaev S. V., Grigorova A. N., Vladimirova O. V., Timofeev S. I., Sirak A. G. [et al.] Influence of connective tissue differentiation on scar tissue formation in children. *Khirurgiya.* 2021;(5):72-77. https://doi.org/10.17116/hirurgia202105172
24. Dodge R. Histological Techniques. *Br. J. Cancer.* 1977. https://doi.org/10.1016/j.etp.2009.02.087

25. Munro B. H. Manual of Histologic Staining Methods of the Armed Forces Institute of Pathology. *Pathology*. 1971. https://doi.org/10.1016/S0031-3025(16)39410-7
26. Abdelrahman T., Newton H. Wound dressings: Principles and practice. *Surgery*. 2011;29:491-495. https://doi.org/10.1016/j.mpsur.2011.06.007
27. Singh S., Young A., McNaught C. E. The physiology of wound healing. *Surg.* 2017;35:473-477. https://doi.org/10.1016/j.mpsur.2017.06.004
28. Broughton G., Janis J. E., Attinger C. E. Wound Healing: An Overview. *Plast. Reconstr. Surg.* 2006;117:1e-S-32e-S. https://doi.org/10.1097/01.prs.0000222562.60260.f9
29. Blinov A. V., Siddiqui S. A., Nagdalian A. A., Blinova A. A., Gvozdenko A. A. [et al.] Investigation of the influence of Zinc-containing compounds on the components of the colloidal phase of milk. *Arab. J. Chem.* 2021;14(7):103229 https://doi.org/10.1016/j.arabjc.2021.103229

About authors:

Elbekyan Karine Sergeevna, DBiolSc, Professor Head of the Department of general and biological chemistry; tel.: +9624007045; e-mail: karinasgma@inbox.ru; https://orcid.org/0000-0003-2403-8663

Blinov Andrey Vladimirovich, PhD, Senior Lecturer of the Department of physics and technology of nanostructures and materials, Faculty of Physics and Technology; tel.: +79187547852; e-mail: blinov.a@mail.ru; https://orcid.org/0000-0002-4701-8633

Blinova Anastasiya Aleksandrovna, PhD, Associate Professor, Associate Professor of the Department of physics and technology of nanostructures and materials, Faculty of Physics and Technology; tel.: +79887679460; e-mail: nastya_bogdanova_88@mail.ru; https://orcid.org/0000-0001-9321-550X

Fedota Natalya Viktorovna, PhD in veterinary medicine, Associate Professor, Therapy and Pharmacology Department of the Faculty of Veterinary Medicine; tel.:+79624429901; e-mail: nataliafedota@yandex.ru; https://orcid.org/0000-0001-9798-1148

Orobets Vladimir Alexandrovich, DVetSc, Professor, Head of the Department of Therapy and Pharmacology of the Faculty of Veterinary Medicine; tel.: +79283276016; e-mail: orobets@yandex.ru; https://orcid.org/0000-0002-4774-263X

Serov Alexander Vladimirovich, DTechnSc, Professor, Professor of the Department of inorganic and physical chemistry, Faculty of Chemistry and Pharmacy; tel.: +79187409135; e-mail: sav_ncstu@mail.ru

UDC 612.123;612.115;616.1
DOI – https://doi.org/10.14300/mnnc.2021.16046
ISSN – 2073-8137

FEATURES OF HIGHLY SPECIFIC FACTORS OF ENDOTHELIAL DYSFUNCTION AND INDICATORS OF THE HEMOSTATIC SYSTEM AND LIPID METABOLISM IN RATS UNDER VARIOUS EXPERIMENTAL CONDITIONS

Tsaturian L. D., Melikbekyan E. O., Dzhandarova T. I., Knyazhetskaya L. O., Baturin V. A., Shchetinin E. V.

Stavropol State Medical University, Russian Federation

ОСОБЕННОСТИ ВЫСОКОСПЕЦИФИЧЕСКИХ ФАКТОРОВ ЭНДОТЕЛИАЛЬНОЙ ДИСФУНКЦИИ, ПОКАЗАТЕЛЕЙ СИСТЕМЫ ГЕМОСТАЗА И ЛИПИДНОГО ОБМЕНА У КРЫС В РАЗЛИЧНЫХ ЭКСПЕРИМЕНТАЛЬНЫХ УСЛОВИЯХ

Л. Д. Цатурян, Е. О. Меликбекян, Т. И. Джандарова, Л. О. Княжецкая, В. А. Батурин, Е. В. Щетинин

Ставропольский государственный медицинский университет, Российская Федерация

This study involved an investigation of lipidogram and coagulogram parameters with assessment of highly specific markers of endothelial dysfunction in 44 Wistar rats under various experimental conditions. Significant intersystem relationships were revealed between the content of circulating endothelial cells and the activated partial thromboplastin time, prothrombin time, platelet count, fractions of atherogenic lipoproteins, and atherogenic coefficient in animal models of hypercoagulation, dyslipidemia, and mild stress.

Keywords: endothelial dysfunction, lipid profile, coagulogram parameters, mild stress, experimental animals

Проведено исследование показателей липидограммы, коагулограммы с оценкой высокоспецифических маркеров эндотелиальной дисфункции у крыс линии Вистар, находящихся в различных экспериментальных состояниях. Выявлены значимые межсистемные взаимосвязи между содержанием циркулирующих эндотелиальных клеток с показателями АЧТВ, протромбинового времени, количеством тромбоцитов, фракциями атерогенных липопротеинов и коэффициентом атерогенности при моделировании у животных гиперкоагуляции, дислипидемии, а также состояния мягкого стресса.

Ключевые слова: эндотелиальная дисфункция, липидограмма, показатели коагулограммы, мягкий стресс, экспериментальные животные